Journal of Hazardous Materials 407 (2021) 124612

Contents lists available at ScienceDirect

Journal of Hazardous Materials

journal homepage: www.elsevier.com/locate/jhazmat

Identification of key residues of carboxylesterase PxEst-6 involved in pyrethroid metabolism in *Plutella xylostella* (L.)

Yifan Li [a,1], Hong Sun [a,1], Zhen Tian [b,1], Yue Li [a], Xuan Ye [a], Ruichi Li [a], Xinyu Li [a], Shengli Zheng [c], Jiyuan Liu [a,*], Yalin Zhang [a,*]

[a] Key Laboratory of Plant Protection Resources & Pest Management of the Ministry of Education, College of Plant Protection, Northwest A&F University, Yangling, Shaanxi 712100, China
[b] College of Horticulture and Plant Protection, Yangzhou University, Wenhui East Road, No. 48, Yangzhou, Jiangsu 225009, China
[c] College of Chemistry & Pharmacy, Northwest A&F University, No. 3 Taicheng Road, Yangling, Shaanxi 712100, China

ARTICLE INFO

Keywords:
Cares
Detoxification
Molecular docking
Site-directed mutagenesis

ABSTRACT

The long-term and excessive use of insecticides has led to severe environmental problems and the evolution of insecticide resistance in insects. Carboxylesterases (CarEs) are important detoxification enzymes conferring insecticide resistance on insects. Herein, the detoxification process of *Plutella xylostella* (L.) carboxylesterase 6 (PxEst-6), one representative *P. xylostella* carboxylesterase, is investigated with cypermethrin, bifenthrin, cyfluthrin and λ-cyhalothrin. RT-qPCR shows that PxEst-6 is highly expressed in the midgut and cuticles of the third instar larvae. Exposure to pyrethroid insecticides resulted in PxEst-6 up-regulation in a short time. Metabolic assays indicate that PxEst-6 has the capacity to metabolize these pyrethroid insecticides. The combination of molecular docking, binding mode analyses and alanine mutations demonstrated that His451, Lys458 and Gln431 were key residues of PxEst-6 for metabolizing pyrethroids and the acetate groups derived from pyrethroids were key sites for being metabolized by PxEst-6. H451- and K458-derived hydrogen bond (H-bond) interactions with the pyrethroid acetate groups and the polar interactions with the pyrethroid acetate group provided by the Q431 sidechain were crucial to the pyrethroids' metabolism by PxEst-6. Our study contributes to revealing the reasons for pyrethroid resistance in *P. xylostella*, and provides a fundamental basis for the development of novel pyrethroid insecticides.

1. Introduction

The diamondback moth, *Plutella xylostella* (L.) (Lepidoptera: Plutellidae), is a cosmopolitan pest attacking cruciferous crops. The annual estimated economic loss resulting from *P. xylostella* has reached 4–5 billion US dollars worldwide (Furlong et al., 2013). Currently, chemical control is still the main method to control *P. xylostella* (Zhu et al., 2019). However, the excessive use of insecticides has caused a surge in insecticide resistance in *P. xylostella* and caused further environmental pollution, even jeopardizing food safety (Sun et al., 2012). As already reported, *P. xylostella* has developed resistance to most insecticide ingredients including organophosphates, carbamates, pyrethroids, and *Bt* toxins (APRD, 2019). Pyrethroids as bionic insecticides have been widely applied in deterring *P. xylostella* (Ray and Fry, 2006). However, *P. xylostella* has been reported to acquire relatively high levels of resistance to pyrethroids including resmethrin, cypermethrin, deltamethrin, fenvalerate, and s-fenvalerate (Liu et al., 1981; Yu and Nguyen, 1992; Sayyed et al., 2008; Zhou et al., 2011). Although pyrethroids show low toxicity to mammals, but they display high toxicity to fishes and non-target invertebrates (Li et al., 2017). The extensive use of pyrethroids has resulted in their massive accumulation in sediment. Currently, pyrethroids has been found residues in sediment in many countries (Food and Agriculture Organization FAO, 2020). For example, the highest concentration of cypermethrin has reached 1140 ng/g dw in sediments in Humber, England (Long et al., 1998). The average concentration of permethrin residue in sediments of Hanoi, Vietnam is 1870 ng/g dw (Hanh Thi et al., 2014). These high concentration of pyrethroids residues is threatening the global eco-system. Therefore, it is important for environmental safety and agricultural health to study the detoxification and metabolism mechanism of *P. xylostella* towards

* Corresponding authors.
E-mail addresses: liujiyuan@nwsuaf.edu.cn (J. Liu), yalinzh@nwsuaf.edu.cn (Y. Zhang).
[1] These authors contributed equally to this work.

https://doi.org/10.1016/j.jhazmat.2020.124612
Received 3 August 2020; Received in revised form 31 October 2020; Accepted 16 November 2020
Available online 9 December 2020

pyrethroids to reduce the usage of pyrethroids.

Carboxylesterases (CarEs) belong to the α/β hydrolase superfamily and are ubiquitous in living organisms (Wheelock et al., 2005). CarEs play an important role in metabolizing xenobiotics and are deemed to be closely associated with the evolution of insecticide resistance in insects (Oakeshott et al., 2010; Oakeshott et al., 2013). This enzyme is related to organophosphate, carbamate and pyrethroid resistance in certain insect species (Newcomb et al., 1997; Feng et al., 2018; Gong et al., 2017; Zhang et al., 2010; Li et al., 2007). Work conducted to date indicates that insect CarEs mediate the development of resistance through gene amplification (increased CarEs expression levels) or mutation (improving the binding capacity of CarEs to insecticides) (Mouches et al., 1986; Claudianos et al., 1999; Campbell et al., 1998; Gu et al., 2013). The gene amplification (the increased expression level) of CarE has been demonstrated to be involved in the increase of resistance in various insects including *Plutella xylostella*, *Myzus persicae*, *Aphis gossypii*, *Bemisia tabaci*, *Helicoverpa armigera*, *Anopheles gambiae*, *Cochliomyia hominivorax*, *Lucilia cuprina* and *Leptinotarsa decemlineata* (Maa et al., 2001; Bizzaro et al., 2005; Cao et al., 2008; Alon et al., 2008; Han et al., 2012; Vontas et al., 2005; de Carvalho et al., 2006; Hartley et al., 2006; Lu et al., 2015). Moreover, the insecticide metabolic capacity of CarEs can be amplified by enzyme mutation, aiding in the acquisition of insecticide resistance (Newcomb et al., 1997; de Carvalho et al., 2006). For example, the mutation of *Lucilia cuprina* esterases (E3 W251L and α7 G137D) was correlated with the organophosphate and pyrethroid resistance, due to their increased capacity to metabolize such insecticides (Newcomb et al., 1997). Recently, the metabolic capacity of insect CarEs has become a great concern. Previous research has found that recombinant insect CarEs have the capacity to metabolize organophosphates and pyrethroids (Teese et al., 2013; Cui et al., 2007).

Although there is a considerable amount of literature indicating that insect CarEs could confer pyrethroid resistance in insects. For CarEs, their binding modes with pyrethroids and key sites essential for pyrethroids metabolism are yet to be clarified.

In this study, we report the function of PxEst-6 in the pyrethroid detoxification metabolism process, and analyze the binding mode of PxEst-6 towards pyrethroids. Our study contributes to the understanding of the molecular mechanism involved in the pyrethroid metabolism by CarEs.

2. Materials and methods

2.1. Insects and chemicals

The susceptible *P. xylostella* population without exposure to any insecticides was maintained in laboratory conditions at 25 °C with 50% relative humidity and 16 L: 8D photoperiod. Larval *P. xylostella* were reared on cabbage (*Brassica oleracea*) which were grown without any pesticide application and were watered regularly. Adults were supplied with a 10% honey solution (insecticide-free). Bifenthrin, cyfluthrin, cypermethrin and λ -cyhalothrin (industrial grade, purity > 98%) were purchased from Topscience (Shanghai, China). Triphenyl phosphate (TPP, an inhibitor of CarE, purity > 99.8%), α-naphthyl acetate (α-NA, purity: 98%), α-naphthol (α-N, purity > 99%) and Fast Blue B Salt were provided by Aladdin (Shanghai, China). All other chemicals or reagents were of the reagent grade and obtained from commercial sources.

2.2. Bioassays

Pyrethroid insecticides (bifenthrin, cyfluthrin, cypermethrin and λ-cyhalothrin) were dissolved in mixed solvent (water: acetone = 4: 1, v/v). The mixed solvent (water: acetone = 4: 1, v/v) without insecticides was used as control. This bioassay method was conducted using the leaf-dipping method (Shelton et al., 1993). The cabbages (*B. oleracea*) were planted in the laboratory without exposure to any insecticides. The cabbage leaves (radius: 2 cm) were immersed in the above-mentioned insecticide solutions or the control group solution for 2–3 s. The soaked leaves were then dried in a fume hood to evaporate the acetone. Afterwards, these leaves were transferred into petri dishes with moist filter paper on the bottom. Ten vigorous *P. xylostella* 3rd instar larvae were introduced to each petri dish and kept in the above-mentioned laboratory conditions. Each assay was replicated three times. The mortality was recorded after 48 h. Larvae without any movement when poked softly with a fine brush were considered as dead. The mortality of the control group was corrected using Abbott's correction (Abbott, 1987). Data for this bioassay were subjected to Probit analysis by SPSS 19.0 (IBM, USA).

2.3. Pyrethroid insecticide exposure

Fifty of the 3rd instar *P. xylostella* larvae were exposed to LC_{10} concentrations (calculated from the results of the bioassay at 48 h) of the four pyrethroids (bifenthrin, cyfluthrin, cypermethrin and λ-cyhalothrin). Control groups were treated with mixed solvent (water: acetone = 4: 1, v/v) without insecticides. The treatment method complied with the previously described leaf-dipping method. Each treatment was replicated three times. At 3, 6, 12, 24 and 48 h, 10 surviving larvae were sampled from each treatment, respectively. The sampled larvae were quick-frozen in liquid nitrogen and stored at −80 °C for the following transcriptional analysis.

2.4. RT-qPCR

The RNAiso Plus (TaKaRA, Japan) was used to extract total RNA from different tissue samples (FB: fat body, CU: cuticle, MG: midgut, HE: head, MT: Malpighian tubule) and insecticide exposure samples followed the manufacturer's instruction. The quality and concentration of extracted RNA were determined by NanoDrop™ 2000 spectrophotometer (Thermo Fisher Scientific, USA), and the RNA integrity was checked by using agarose gel electrophoresis. The cDNA for RT-qPCR was obtained by using EasyScript® One-Step gDNA removal and cDNA synthesis SuperMix (TransGen, China) following the attached protocol. The specific primers of RT-qPCR were designed by employing online primer tool (Integrated DNA Technologies primer quest tool, https://sg.idtdna.com/PrimerQuest/Home/Index) (Table S1). A total of 20 μL RT-qPCR reaction system contained 0.4 μL of forward and reverse primers, 10 μL Tip Green qPCR SuperMix (TransGen, China), 1 μg cDNA temple and variable nuclease-free water. The amplification parameters of the RT-qPCR reaction were set as follows: started at 94 °C for 5 min, followed by 45 cycles consisting of 94 °C for 5 s and 56 °C for 30 s, then generating a melting curve on LightCycler®480 (Roche, Switzerland). The obtained PCR products were determined by 1% agarose gel electrophoresis detection. A standard curve using serial 10-fold dilutions of the cDNA template was established to determine the amplification efficiency. RNase-free water replaced cDNA template as the negative control. Three biological and three technical replications were performed for each gene. The relative expression levels were calculated according to $2^{-\Delta\Delta Ct}$ method (Livak, 2001) with elongation factor 1 (*EF-1*) and ribosomal protein L32 (*RPL32*) as reference genes. Data for the transcriptional expression level of the PxEst genes were analyzed in Prism 6.0 (Graphpad, USA) using a one-way ANOVA analysis and Tukey's multiple comparison test.

2.5. Gene synthesis and site-directed mutagenesis

The gene sequence of PxEst-6 (GenBank ID: HQ199328) containing ingestion sites (BamH I and Hind III) was synthesized by Sangon Biotech (Shanghai, China). Site-directed mutagenesis of H451A, K458A, Q431A and L324A in PxEst-6 were performed by using the *Fast Mutagenesis* System (Cat#: FM111-01, TransGen, China) according to the manufacturer's protocol. The specific primers for site-directed mutagenesis were designed in accordance with the manufacturer's instructions provided

by the *Fast Mutagenesis* System (Cat#: FM111-01, TransGen, China).

2.6. Expression and purification of PxEst-6

The PxEst-6 and its mutant genes were inserted into *pET-32a* (+) to construct the expression vectors. The constructed expression vectors were transformed into competent BL21 (DE3) strains of *E. coli*. The positive transformants were cultured in 500 mL LB medium (encompassing a final concentration of 100 μg/mL ampicillin). To induce the cultures, a final concentration of 0.6 mM D-Sorbitol and 0.1 mM isopropyl-β-D-thiogalactopyranoside (IPTG) were added into the medium when OD_{600} reached 1.2, followed by shaking at 200 rpm at 16 °C for 24 h. The cells were harvested by centrifugation at 4 °C, 8000 g for 10 min. Cell pellets were re-suspended in 10 mL PBS (10 mM, pH 7.4) and lysed by ultrasonication of 250 W (Sonics, USA) for 10 min on ice (10 s work and 10 s stop). After centrifugation at 4 °C, 12,000 g for 30 min, the supernatant was collected and loaded onto a purification Ni-NTA spin column (Yeasen, China). The recombinant protein was then eluted using a serial dilution of imidazole (50–250 mM). The target proteins were detected using 12% SDS-PAGE. The purified target proteins were ingested by enterokinase to obtain the Trx-free recombinant protein and dialyzed overnight in Tris-HCl / $CaCl_2$ buffer (25 mM / 1 mM, pH 7.4). The concentration of proteins was determined by the BCA method.

2.7. Enzymatic activity and enzyme inhibition assays

The activity of PxEst-6 and its mutants were evaluated using α-NA as substrate in a 96-well microplate and absorbance was monitored by a microplate reader (M200 PRO, Switzerland) (Grant et al., 1989). The standard curve of α-N was constructed using the OD_{600} of different α-N concentrations (9.375, 18.75, 37.5, 75, 150 and 300 μM). In the enzyme activity assay, the 100 μL protein diluent (containing 1 μg recombinant protein, Tris-HCl/$CaCl_2$ buffer, pH 7.4) and six different concentrations of α - NA (25 μM-250 μM) were incubated for 10 min at 30 °C. Then 100 μL coloring solution (containing 1% Fast Blue B Salt 5% SDS 2:5 v/v) was added into the protein diluent for the color reaction. After 30 min, the absorbance of the reaction mixture at 600 nm was detected and quantitatively analyzed based on the α-N standard curve. Each assay was performed three times. The control groups used a heat-inactive protein in the place of a recombinant protein. Enzyme activities were shown as $nmol^{-1}$ min^{-1} μg^{-1}. The obtained enzyme activities at different concentrations of α-NA were plotted in GraphPad Prism 6.0 (GraphPad, USA) using the Enzyme-kinetics model to calculate the K_m and V_{max}. Inhibition assays were conducted following the previously reported method (Cui et al., 2007). Serial dilutions of bifenthrin, cyfluthrin, cypermethrin and λ -cyhalothrin were co-incubated with 1 μg recombinant protein for 10 min before the addition of substrate α-NA. The residual activity of PxEst-6 and its mutants were determined according to the above-mentioned enzyme activity assay method.

2.8. Insecticide hydrolysis assays

The hydrolytic capacity of PxEst-6 and its mutants towards pyrethroid insecticides (bifenthrin, cyfluthrin, cypermethrin and λ -cyhalothrin) were performed in glass test tubes. The reaction system was composed of 0.5 mM of the above-mentioned insecticides, 20 μg PxEst-6 or its mutant proteins, and Tris-HCL/$CaCl_2$ (pH 7.4). The reaction mixtures were shaken at 200 rpm/min, 30 °C for 2 h in glass test tubes before adding 500 μL methanol (HPLC-grade) to terminate the reactions. Control groups contained heat-inactive proteins (PxEst-6 or its mutant proteins). The hydrolytic capacity of PxEst-6 and its mutants were evaluated by using ultra-high-performance liquid chromatography (UPLC) (Shimadzu, Japan) equipped with a C18 column. Standard bifenthrin, cyfluthrin, cypermethrin and λ -cyhalothrin were separated using the chromatographic separation reversed-phase high-pressure liquid chromatography to determine their peak location. The chromatographic conditions were as followings: The column temperature was kept at 30 °C. The mobile phase consisted of 30% methanol and 70% water to separate the insecticides, and the detection absorbance wavelength was 235 nm. Flow rate was 0.8 mL/min. After locating the peaks of the applied pyrethroid insecticides, the earlier mentioned reaction mixtures were transferred into the sample vials and were subjected to UPLC detection following chromatographic conditions as described above. Data were analyzed by a one-way ANOVA followed with Tukey's multiple comparison test.

2.9. Structural modeling of PxEst-6

Taking the crystal structure of *Aspergillus niger* EstA (PDB ID: 1ukc: A) as the template for homology modeling, the 3D model of PxEst-6 was built using Modeller 9.10 (Šali and Blundell, 1993; Schrag and Cygler, 2004). The alignment between sequences of PxEst-6 and *A. niger* EstA was generated by Align2D. Thereafter, 1000 3D models of the PxEst-6 were calculated automatically. Each model was initially optimized by the variable target function method (VTFM) with conjugate gradients (CG), followed by refinement based on molecular dynamics (MD) with simulated annealing (SA). Conformations of the loops in PxEst-6 models were refined using the Loopmodel in Modeller software. The stability of PxEst-6 conformation was measured by the GA341 and Discrete optimized protein energy (DOPE) scores. The conformation with the lowest DOPE energy was taken as the credible structure of PxEst-6. The quality of the credible PxEst-6 conformation was further assessed by Molprobity and Profile 3D (Chen et al., 2010; Liu et al., 2014; Tian et al., 2019).

2.10. Molecular dynamics (MD) simulations

All molecular dynamics simulations were performed with the software Cresset Flare (Flare, 4.0.2, Cresset®, Litlington, Cambridgeshire, UK) (Flare; Cheeseright et al., 2006; Bauer and Mackey, 2019; Kuhn et al., 2020). For PxEst-6 and the four pyrethroids, the GAFF and the AM1-BCC method were employed to set the pyrethroids' parameters and charges, the bioorganic systems force field in AMBER was chosen to depict the PxEst-6 protein parameters (Jakalian et al., 2002; Hummer et al., 2001). Before MD simulations, the energy minimization for each complex was performed to eliminate unfavorable contacts. Each solvated complex was then equilibrated without unrestraint for 200 ps at 300 K and constant pressure. The production phase was run for 10 ns using the same conditions as the equilibration phase to prevent an abrupt jump in the potential energy. MD results were analyzed with Ambertools13 package (Case et al., 2010). All the detail of MD simulations was performed according to our former reports (Tian et al., 2019, 2020; Liu et al., 2018).

2.11. Molecular docking simulations

Molecular docking of the 4 pyrethroids (bifenthrin, cyfluthrin, cypermethrin, and λ-cyhalothrin) with PxEst-6 was simulated by the program GOLD 2020.1 (Jones et al., 1995, 1997). The binding pocket of the PxEst-6 was located using the Metapocket2.0 pocket prediction algorithm. The top one pocket generated by Metapocket2.0 was defined as the centroid of the binding site with 10 Å radius sphere. For the 4 pyrethroids, their 3D structures were sketched using Marvinsketch (Chemaxon Inc.) and optimized for 2000 steps in Amber18 with the GAFF force field (Wang et al., 2004; Case et al., 2010). The PxEst-6 structure produced by homology modelling was used as the receptor of pyrethroids after a 5000-step energy minimization in Amber18 with the ff99SB force field (Wang et al., 2004; Hummer et al., 2001). Due to the superiority of in predicting ligand binding pose, a ChemPLP score was utilized to predict the most accurate binding modes of the 4 pyrethroids (Chen et al., 2014; Tian et al., 2016a). All structures were visualized using the PyMol 1.3r1 edu software (DeLano, 2002).

2.12. Binding energy calculations

For each of the 4 pyrethroids, the docking pose possessing the highest ChemPLP score was reevaluated by the Chemscore to estimate the binding free energy (ΔG) (Chen et al., 2014; Baxter et al., 1998; Eldridge et al., 1997; Tian et al., 2016b). In Chemscore, the ΔG was calculated using Eq. (1):

$$\Delta G_{binding} = \Delta G_O + \Delta G_{hbond} + \Delta G_{lipo} + \Delta G_{rot} \quad (1)$$

The Chemscore function in our work can be written in the form:

$$\Delta G = -5{\cdot}4800 + -3{\cdot}3400*S\ (\text{hbond}) + -0{\cdot}1170*S\ (\text{lipo}) + 2{\cdot}5600*H\ (\text{rot}) \quad (2)$$

Each component of this equation is the product of a term depending on the magnitude of a particular physical contribution to free energy (e.g. hydrogen bonding).

2.13. Statistics analysis

The depletion rate was calculated by the formula (3):

$$\text{Depletion of Pyrethroids}(\%) = \frac{\text{Peak area C} - \text{Peak area T}}{\text{Peak area C}} \times 100 \quad (3)$$

In formula (3), peak C represents the peak area of the control group and peak T represents the peak area of the treated group.

The depletion ratio was determined by the formula (4):

$$\text{Depletion ratio} = \frac{\text{Depletion rate T}}{\text{Depletion rate C}} \quad (4)$$

In formula (4), depletion rate C represents the depletion rate of pyrethroids of the control group, and depletion rate T represents the depletion rate of pyrethroids in the treated group.

3. Results and discussion

3.1. Toxicity of pyrethroids against P. xylostella

Pyrethroids, as inhibitors of the sodium channel, are widely used in the control of *P. xylostella*. In this study, the ingestion toxicity (48 h) of bifenthrin, cyfluthrin, cypermethrin and λ -cyhalothrin on the 3rd instar larvae of *P. xylostella* was obtained by using the leaf-dipping method. As shown (Table 1), the toxicity of these four pyrethroids were similar to previous reports (Liu et al., 2003; Yi et al., 2016). The LC_{50} values of bifenthrin, cyfluthrin, cypermethrin and λ -cyhalothrin were 14.54 mg/L, 9.87 mg/L, 7.35 mg/L and 4.63 mg/L, respectively. The corresponding LC_{10} values were 4.51 mg/L, 1.27 mg/L, 2.30 mg/L and 0.97 mg/L, respectively (Table 1). These results illustrate that the *P. xylostella* strain shows high sensitivity to pyrethroids in this study, and determined the LC_{10} dosage for following insecticide exposure assay.

3.2. Tissue-specific expression patterns of PxEst-6

The expression of insect CarEs is tissue-specific, and the expression patterns of different CarEs genes in different tissues of insects may represent their biological functions (Yu et al., 2009; Tsubota and Shiotsuki, 2010). We analyzed the tissue-dependent expression of PxEst-6 in five tissues (fat body, cuticle, head, midgut and Malpighian tubule) by RT-qPCR. Insect CarEs are important detoxification enzymes closely related to the development of insecticide resistance, so they are usually abundant in the feeding and digestive tissues. As expected, PxEst-6 was highly expressed in the cuticle and midgut of *P. xylostella* among all the tissues (Fig. 1). To the best of our knowledge, insect midgut is the first barrier to resist the peroral toxicity of insecticides and is usually rich in various detoxification enzymes including CarEs (Zhang et al., 2013). In this study, PxEst-6 was highly expressed in *P. xylostella* midgut, suggesting PxEst-6 may be involved in the detoxification of peroral toxicity. Additionally, the cuticles are known as the primary shields to protect insects from xenobiotics (Wan et al., 2016). The high expression of PxEst-6 in the *P. xylostella* cuticles suggested that PxEst-6 may function to block the penetration of insecticides into the insect body. Our speculations on the functions of PxEst-6 in tissues are consistent with the action modes of pyrethroids (Soderlund, 2008). Thus, it is reasonable to speculate that PxEst-6 possibly participates in the detoxification of pyrethroids in *P. xylostella*.

Table 1
Toxicity of pyrethroids against *P. xylostella* over 48 h.

Insecticide	Slope±SE	χ^2	LC_{10} (95% confidence interval) mg/L	LC_{50} (95% confidence interval) mg/L
Bifenthrin	2.51 ± 0.73	6.32	4.51(2.62–7.03)	14.54(9.77–19.53)
Cyfluthrin	1.97 ± 0.66	7.14	1.27(0.74–1.86)	9.87(6.34–12.68)
Cypermethrin	1.63 ± 0.41	8.15	2.30(1.49–3.64)	7.35(4.57–10.36)
λ-cyhalothrin	1.27 ± 0.23	5.87	0.97(0.55–1.53)	4.63(2.19–6.49)

3.3. Expression profile of pyrethroid exposure

Under the LC_{10} dosage of pyrethroid exposure, the mRNA expression level of PxEst-6 shows a significant time-dependent increase (Fig. 2). As shown in Fig. 2, the significant increase of PxEst-6 can be observed from 3 h after the pyrethroid exposure. After exposure to the four pyrethroids for 12 h, the expression levels of PxEst-6 was up-regulated 9.88-, 11.68-, 13.57- and 10.81-fold which were the most significant up-regulations during the exposure time. Then the up-regulation trends recede (Fig. 2). It should be noted that the four pyrethroid's mediated variation trends of PxEst-6 expression were identical in the whole exposure time. It was reported that the up-regulated genes resulting from insecticide exposure were generally associated with the detoxification metabolism of insecticides (Oakeshott et al., 2013; Lyubimov, 2011). Previous research indicates that insecticides could induce the upregulated expression of CarEs in *Bombyx mori*, *Aphis gossypii*, and *Panonychus citri* in a short time, suggesting these upregulated CarEs genes were involved in the insecticide's detoxification (Gu et al., 2013; Zhang et al., 2013; Wan et al., 2016). Additionally, the overexpression of CarEs can increase the metabolic capacity of insects towards pyrethroids, thereby resulting the development of insecticide resistance (Li et al., 2007; Soderlund, 2008). Likewise, this study found that the four pyrethroids could cause the up-regulation of PxEst-6 in a fairly short time. These results indicate PxEst-6 might play a pivotal role in metabolizing pyrethroids directly in

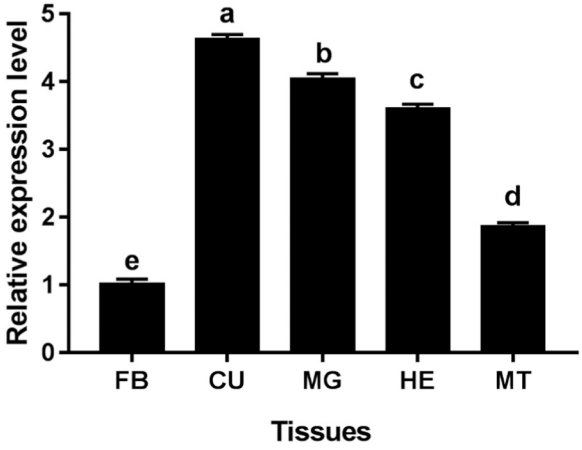

Fig. 1. The expression level of PxEst-6 in different tissues. FB: fat body, CU: cuticle, MG: midgut, HE: head, MT: Malpighian tubules. The results are shown as the mean ± SD. The error bars represent the standard errors calculated from three replicates. Different letters above bars represent statistically significant differences by one-way ANOVA, post-hoc test by Tukey ($P < 0.05$).

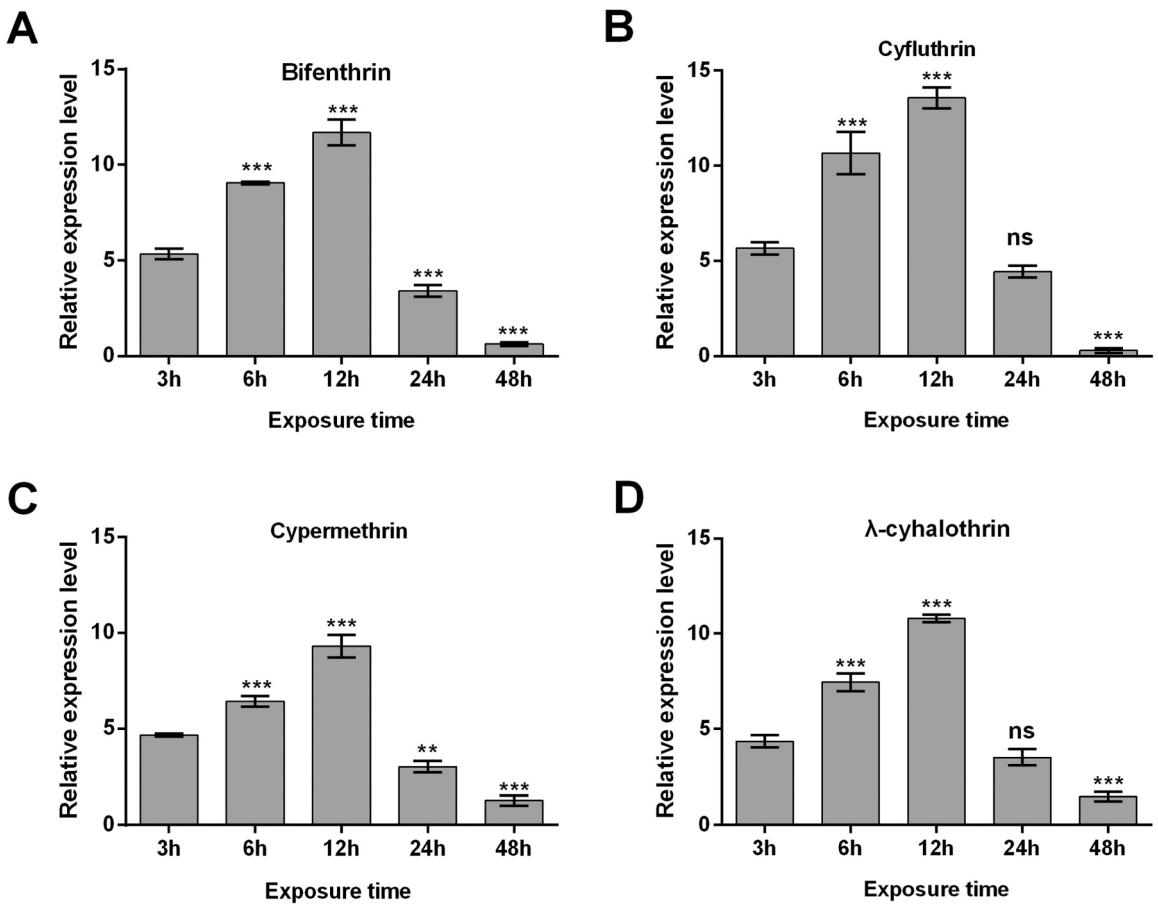

Fig. 2. The expression level of PxEst-6 exposure to LC_{10} of Bifenthrin (A), Cyfluthrin (B), Cypermethrin (C), and λ-cyhalothrin (D). The results are shown as the mean ± SD. The expression levels were normalized to the reference genes EF-1 and RPL-32. Asterisks above represent statistically significant differences by one-way ANOVA, post-hoc test by Tukey (***$P \leq 0.001$, ns: no significance).

P. xylostella. Furthermore, we infer that PxEst-6 is likely to be associated with pyrethroid resistance of *P. xylostella.*

3.4. Inhibition and metabolism assays

The recombinant PxEst-6 protein was prepared to verify the involvement of PxEst-6 in detoxifying pyrethroids. As displayed by SDS-PAGE, the band of recombinant PxEst-6 protein just fell within the expected region (Fig. S1). The catalytic kinetic parameters of the recombinant PxEst-6 protein towards α-Na were determined by Michaelis-Menten equation, with K_m, V_{max}, and k_{cat} being 87.16 μM, 196.1 nM^{-1} mg^{-1} min^{-1}, and 9.85 s^{-1}, respectively (Fig. S3). These results show that the purified recombinant protein PxEst-6 had a higher purity and activity.

To further verify the biochemical characteristics of PxESt-6 towards pyrethroids, an in vitro inhibition assay and a metabolism assay were performed. We initially determined the inhibitory effect of the four pyrethroids on the recombinant PxEst-6 recombinant protein (using TPP as a positive control). As shown, the IC_{50} of TPP was 0.31 mM (Fig. S2). Compared to TPP, all four pyrethroids show lower inhibitory effects on PxeEst-6, with no inhibition rates exceeding 15% at 1 mM. We further tested the metabolic capacity of purified PxEst-6 protein on the four pyrethroids by UPLC. For the four pyrethroids (bifenthrin, cyfluthrin, cypermethrin and λ -cyhalothrin), their 2 h metabolism rates by PxEst-6 reached 40.50%, 32.33%, 22.67% and 26.71%, respectively (Fig. 3).

Metabolizing exogenous substances such as insecticides is one of the important functions of insect CarEs. A number of studies have reported that insect CarEs can metabolize a variety of insecticides including

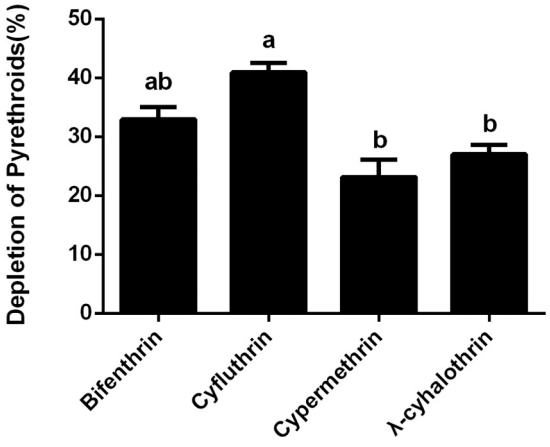

Fig. 3. Metabolic capacity of PxEst-6 towards pyrethroids. The metabolic capacity of PxEst-6 is shown as depletion of pyrethroid. The percentage of pyrethroid cleared by 20 μg wild-type (WT) protein at 30 °C for 2 h is indicated by pillar height. Heat-inactivated proteins were used as control. Error bars represent mean ± SD. Different letters on bars indicate the significant differences by one-way ANOVA, post-hoc test by Tukey.

pyrethroids (Wang et al., 2018; Lan et al., 2005). However, investigations on the insecticide detoxification by *P. xylostella* CarEs are quite limited. In previous reports, carboxylesterase 001G in *Helicoverpa armigera* could metabolize 28% of λ-cyhalothrin and 18% of β-cypermethrin in 2 h (Li et al., 2020). Additionally, carboxylesterase 001H

could degrade 18% of λ-cyhalothrin and 36% of β-cypermethrin (Bai et al., 2019). Carboxylesterase of *Rhopalosiphum padi* (L.) could metabolize 30% of cyhalothrin (100 μM) in 30 min. The metabolic capability of our recombinant CarE (PxEst-6) was similar to these reported insect CarEs (Wang et al., 2018). Our results demonstrate that PxEst-6 could hydrolyze bifenthrin, cyfluthrin, cypermethrin and λ -cyhalothrin with different efficiencies. The different chemical structures of the four pyrethroids is speculated to be responsible for the metabolic differences of PxEst-6 towards the four pyrethroids in this study. Previous research has found that insecticides (paraoxon-ethyl, parathion-methyl, chloropyrifos) with strong competitive inhibition on CarEs are not easy to be metabolized by CarEs, but insecticides (β-cypermethrin, λ-cyhalothrin and fenvalerate) with weak inhibition on CarEs are more likely to be metabolized (Bai et al., 2019). Similar phenomena have likewise been found in this study. The above results demonstrate that these four pyrethroids can be metabolized by PxEst-6. Meanwhile, the four pyrethroids could not effectively inhibit the hydrolysis capacity of PxEst-6 towards α - Na at 1 mM. Therefore, we speculate that the inhibitory capacity of insecticides on insect CarEs does not reflect the metabolic capacity of CarEs. This may due to the inhibitory effects of insecticide on CarE and that the metabolic effects of CarE towards insecticides occur in different domains of CarE.

3.5. Binding mode and molecular dynamics simulations analysis

Binding modes of the four pyrethroids (bifenthrin, cyfluthrin, cypermethrin, and λ-cyhalothrin) were analyzed based on molecular docking. As shown (Fig. 4A), these pyrethroids bound similarly in the PxEst-6 cavity composed of one hydrophobic residue (Leu324) and three hydrophilic residues (Gln431, His451, and Lys458). For bifenthrin, the cresyl and phenyl parts of the 2-methylbiphenyl group were 4.75 Å and 6.2 Å away from the Leu324 CG atom; hydrophobic contacts were detected between them (Fig. 4A). Meanwhile, the carbonyl oxygen atom in the bifenthrin acetate group formed a hydrogen bond (H-bond) interaction with the NE2 atom in the His451 sidechain, with the H-bond distance being 3.3 Å (Fig. 4A). The close distance between Gln431 (a negative-charged residue) and bifenthrin acetate group resulted in a significant polar interaction. The halogen bond (3.7 Å) occurred between the fluorine atom of bifenthrin trifluoromethyl and the NZ atom of the Lys458 sidechain should not be neglected as well.

The cyfluthrin was distinguished from cypermethrin by the extra fluorine atom (F) substitution on the phenyl of the phenoxyphenyl group. It is this tiny structural difference that causes the different orientations of cyano and carbonyl oxygen in these two pyrethroids (Fig. 4B and C). The cyfluthrin cyano generally formed hydrophobic contacts with the Leu324 sidechain and polar interactions with the amido of Gln431 sidechain (N-N distance: 4.7 Å) (Fig. 4B). As for the carbonyl oxygen of the cyfluthrin acetate group, it interacted with the NZ atom of the Lys458 sidechain through an H-bond (3.0 Å) (Fig. 4B). Notably, the centroid of the F-containing phenyl in the cyfluthrin phenoxyphenyl group was only 4.7 Å and 4.4 Å away from the imidazole ring of His451 and NZ atom of the Lys458 sidechain, respectively. As a result, the same F-containing phenyl occurred cation–π interactions with these two positively charged residues (Fig. 4B). In the PxEst-6-cypermethrin complex (Fig. 4C), the hydrophobic contacts between the phenoxyphenyl group and Leu324 became fairly weak due to their distance (7 Å). The H-bond interaction between cypermethrin cyano and the Gln431 sidechain was enhanced, with N-N distance of 2.7 Å (Fig. 4C). The lack of F made the two phenyls of cypermethrin phenoxyphenyl group more flexible. As a result, both these two phenyls were involved in the cation–π interactions with His451 and Lys458. As shown in Fig. 4C, the imidazole ring of the His451 sidechain was 5.2 Å away from the centroid of the phenoxyphenyl group terminal phenyl, and the NZ atom of Lys458 was 5.2 Å away from the centroid of the other phenoxyphenyl phenyl.

Viewed from chemical structure, λ-cyhalothrin is a bioisosteric

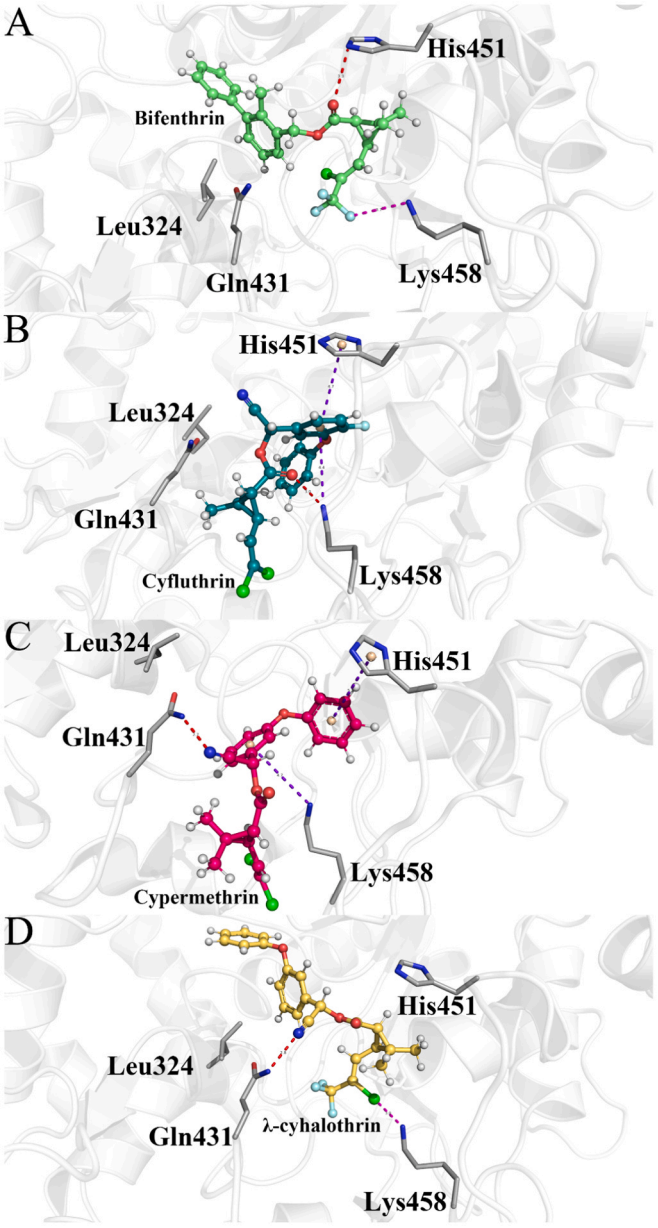

Fig. 4. Binding modes (A) bifenthrin, (B) cyfluthrin, (C) cypermethrin, and (D) λ-cyhalothrin in the cavity of PxEst-6. The four pyrethroids are presented with the stick-and-sphere model. Bifenthrin color code: green, C; red, O; light green, F; white, H. Cyfluthrin color code: cyan, C; red, O; blue, N; green, Cl; white, H. Cypermethrin color code: magenta, C; red, O; blue, N; green, Cl; white, H. λ-cyhalothrin color code: yellow, C; red, O; blue, N; light green, F; green, Cl; white, H. Key residues in the active site of PxEst-6 were presented with the stick model. Color code: gray, C; red, O; blue, N. Red dashed line, H bond. Magenta dashed line, Halogen bond. Purple blue dashed line, Cation–π interaction. (For interpretation of the references to colour in this figure legend, the reader is referred to the web version of this article)

replacement product of cyfluthrin, being produced by replacing the chlorine atom (Cl) in the cyfluthrin dichloroethenyl group. However, the binding pose of λ-cyhalothrin is closer to that of bifenthrin, due to the high similarity of their molecular shapes (Fig. 4A and D). Similar to the bifenthrin biphenyl, the λ-cyhalothrin phenoxyphenyl group could establish remarkable hydrophobic contacts with Leu324. The distance between the CG atom of Leu324 and the two phenoxyphenyl phenyls were 4.75 Å and 6.15 Å, respectively (Fig. 4D). Differences between the binding modes of bifenthrin and λ-cyhalothrin were observed as well. An

H-bond in the PxEst-6-λ-cyhalothrin complex was detected between the N atom of cyano and the N atom of the Gln431 sidechain, with an N-N distance of 2.8 Å. For the acetate group of λ-cyhalothrin, it only occurs with polar interaction with the His451 sidechain (Fig. 4D). Moreover, the halogen bond in the PxEst-6-λ-cyhalothrin complex was shorter than its counterparts in the PxEst-6-bifenthrin complex, due to the closer distance (3.0 Å) between Cl of λ-cyhalothrin and Lys458.

To better elucidate binding modes between PxEst-6 and 4 pyrethroids, the complexes formed by PxEst-6 and 4 pyrethroids through molecular docking were subjected to molecular dynamics (MD) simulations. In the course of 10 ns MD simulations, the PxEst-6-Bifenthrin, PxEst-6-Cyfluthrin, PxEst-6-Cypermethrin, and PxEst-6-Cyhalothrin complexes all achieved equilibrium at about 2 ns with an averaged root-mean-square deviation (RMSD) of the backbone atoms being 3.34 ± 0.31 Å, 3.26 ± 0.39 Å, 4.05 ± 0.44 Å, and 3.62 ± 0.34 Å, respectively(Fig. 5). Such a rapid equilibrium suggested stability of the complexes formed by the PxEst-6 and these 4 pyrethroids (Fig. 5). Binding stability of the four pyrethroids to PxEst-6 can also be embodied in the dynamic video showing 10 ns MD trajectories of corresponding complexes (SI Movie).

Supplementary material related to this article can be found online at doi:10.1016/j.jhazmat.2020.124612.

3.6. Alanine mutations reveal the key residues involved in 4 pyrethroid metabolisms

Based on the results of the aforementioned binding mode analysis, four residues (Leu324, Gln431, His451, and Lys458) were individually replaced by Ala to determine their key interactions with chemical groups of the four pyrethroids (bifenthrin, cyfluthrin, cypermethrin, and λ-cyhalothrin). The effects of these residues on the metabolism of pyrethroids by PxEst-6 were also analyzed by UPLC.

Even though bifenthrin and λ-cyhalothrin possessed similar binding modes, the residue mutation exerted different effects on their metabolism. When replacing the Lys458 of PxEst-6 with Ala (PxEst-6K458A), the metabolism efficiency of λ-cyhalothrin was reduced 50%, while the counterpart of bifenthrin exhibited no significant change (Fig. 6A and D). This indicates that the Lys458-derived halogen bond in the PxEst-6-bifenthrin complex is not as important as that in the PxEst-6-λ-cyhalothrin complex. The mutation of Gln431 (PxEst-6Q431A) dismissed the polar interaction with the bifenthrin acetate group and the H-bond interaction with λ-cyhalothrin cyano, decreasing the metabolism efficiency of bifenthrin and λ-cyhalothrin by 50%, suggesting the key role of Gln431 in metabolizing bifenthrin and λ-cyhalothrin (Fig. 6A and D). His451 is involved in interacting with the acetate groups in bifenthrin and λ-cyhalothrin; its mutation (PxEst-6H451A) could result in the significantly reduced metabolism of these two pyrethroids. Meanwhile, a more substantial capacity reduction of PxEst-6H451A in metabolizing bifenthrin was observed (Fig. 6A and D). Considering the differences of His451 in interacting with the two acetate groups, it is reasonable to state that the His451-derived H-bond outweighs His451-derived polar interactions in pyrethroid metabolism. Replacing Leu324, the residue interacting with the phenyl groups of bifenthrin and λ-cyhalothrin through hydrophobic contacts caused no significant change of pyrethroid metabolism by PxEst-6.

The binding modes of cyfluthrin and cypermethrin are also similar. In the PxEst-6-cyfluthrin complex, Lys458 occurred H-bond interaction and cation–π interaction with the acetate carbonyl and phenoxyphenyl phenyl of cyfluthrin, respectively (Fig. 4B). While in the complex formed by PxEst-6 and cypermethrin, the Lys458-derived interactions with the acetate carbonyl and phenoxyphenyl phenyl of cypermethrin became polar interaction and cation–π interaction (Fig. 4C). As shown in Fig. 5B and C, the replacement of Lys458 (PxEst-6K458A) exerted more negative effect on the metabolism of cyfluthrin, suggesting that the H-bond formation between Lys458 and acetate carbonyl of cyfluthrin are key to maintaining the cyfluthrin-metabolizing ability of PxEst-6. The cyfluthrin-metabolizing ability of PxEst-6 is greatly reduced by the mutation of Q431, indicating the key role of the Q431-derived polar interaction with the cyfluthrin acetate group in the cyfluthrin metabolism by PxEst-6 (Fig. 6B). Whereas for cypermethrin, its metabolism was much less affected by the Q431 mutation, even though an H-bond is formed between Q431 and cypermethrin cyano (Fig. 6C). As revealed by the much decreased efficiency of PxEst-6H451A in metabolizing cyfluthrin and cypermethrin (Fig. 6B and C), the cation–π interaction provided by H451 was key to the metabolism of these two pyrethroids. For L324, its mutation showed little influenced on the metabolism of cyfluthrin and cypermethrin by PxEst-6 (Fig. 6B and C), further suggesting the futility of L324-derived hydrophobic contacts in metabolizing cyfluthrin and cypermethrin.

Based on above analysis, it can be speculated that the metabolism site of these four pyrethroids may occur at the site of their acetate groups. The His451- and Lys458-derived H-bond interactions with the pyrethroid acetate groups are crucial to the pyrethroids metabolism by PxEst-6. The polar interactions with pyrethroid's acetate group provided by the Q431 sidechain should be a concern as well. The hydrophobic interaction derived from L324 works to stabilize the pyrethroids in the binding pocket of PxEst-6, aiding the Q431, H451 and K458 interacting with the pyrethroid acetate groups. According to these discoveries, whether the acetate groups of pyrethroid analogs formed polar interactions or H-bond interactions with the sidechains of Q431, H451 and K458 can be taken as key indicators when designing novel pyrethroid analogs based on the chemical scaffold of current pyrethroids. What should be kept would be those pyrethroid analogs occurring with no such interactions with Q431, H451 and K458 sidechains. More radically, replacing the pyrethroid acetate groups with bioisosteric groups characterized by nonpolarity and no H-bond acceptor could directly remove the interactions of novel pyrethroid analogs with these three residues, thus improving the insecticidal activity of novel pyrethroids by remitting PxEst-6 metabolism.

4. Conclusion

In summary, the present study corroborated that PxEst-6 has the potential to be involved in the detoxification metabolic process of the four pyrethroids (bifenthrin, cyfluthrin, cypermethrin,and λ-cyhalothrin) in *P. xylostella*. Combining the results of binding modes analysis and alanine mutations, it is indicated that the metabolism site of these four pyrethroids may occur at the site of their acetate groups, and the residues Q431, H451 and K458 of PxEst-6 play crucial roles in pyrethroid metabolism.

Based on the above-mentioned results, we suggest that reducing or eliminating the activity of CarEs can be applied to mitigate the resistance of *P. xylostella* against pyrethroid. Additionally, to develop novel pyrethroids as insecticides, replacing acetate groups in pyrethroid with it bioisosteric groups characterized by nonpolarity and no H-bond acceptor is suggested. In this way, the possibility of insecticides metabolized by CarEs can be decreased, thereby enhancing the insecticidal activity.

Funding

This research was supported by the Fundamental Research Funds for the Central Universities (2452018008), the Key Research & Development Project of Shaanxi Province (2019NY-186), the Sci-Tech Planning Project of Yangling Demonstration Zone (2018NY-02), and the National Natural Science Foundation of China (21503272, 31872012).

Credit authorship contribution statement

Yalin Zhang and **JiYuan Liu**: Conceptualization, Supervision, Funding administration, Writing - review & editing. **Yifan Li, Hong Sun** and **Zhen Tian**: Investigation, Methodology, Data curation, Formal

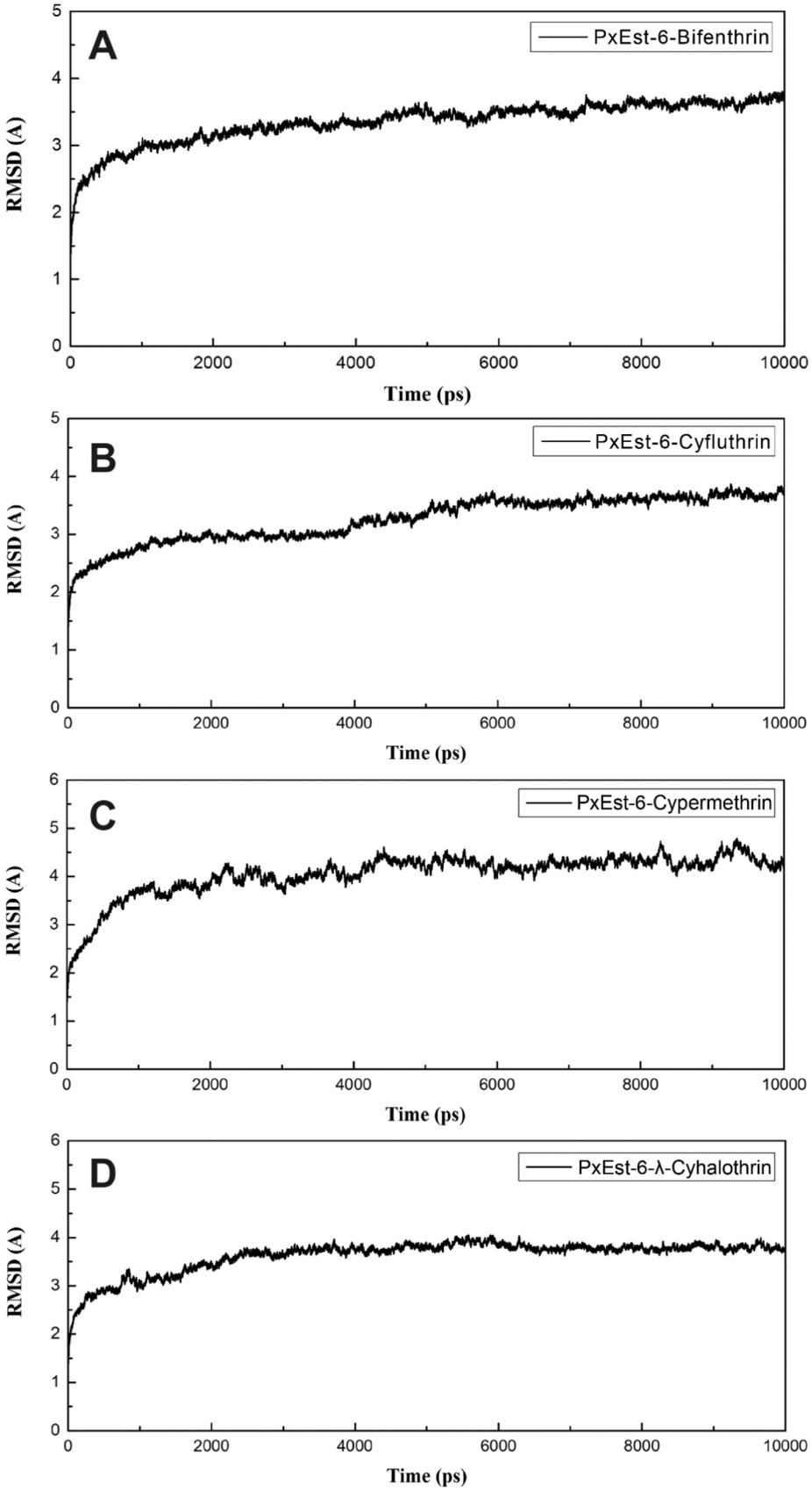

Fig. 5. RMSD values for the PxEst-6-Bifenthrin, PxEst-6-Cyfluthrin, PxEst-6-Cypermethrin, and PxEst-6-Cyhalothrin complexes structures monitored during the 10 ns production phase MD simulations.

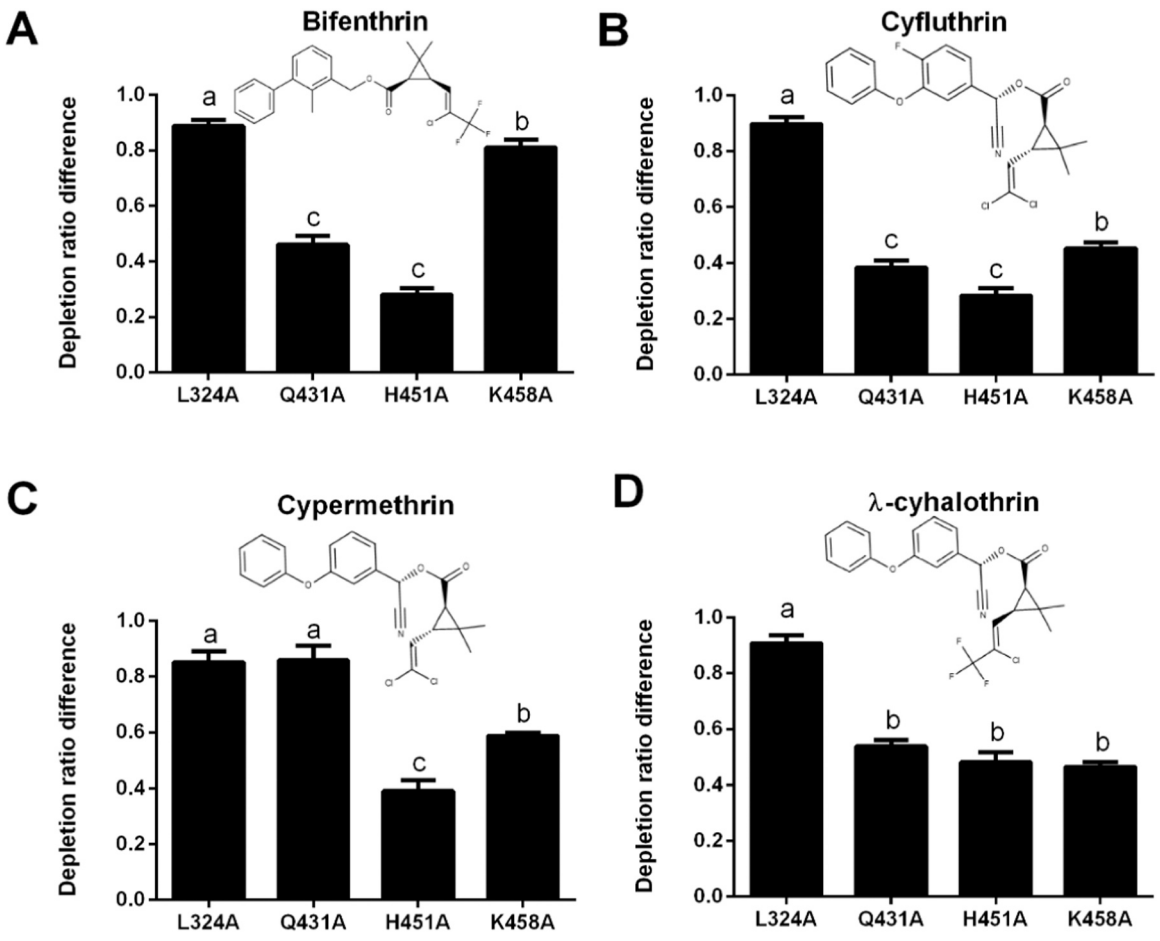

Fig. 6. Depletion ratio of PxEst-6 mutant protein compared to wide type protein. (A) Bifenthrin, (B) Cyfluthrin, (C) Cypermethrin, and (D) λ-cyhalothrin. Error bars represent mean ± SD. Different letters on bars indicate the significant differences by one-way ANOVA, post-hoc test by Tukey.

analysis, Visualization, Validation, Software, Writing - original draft. **Yue Li, Xuan Ye, Ruichi Li, Xinyu Li** and **Shengli Zheng**: Investigation, Visualization.

Declaration of Competing Interest

The authors declare no conflict of interest.

Acknowledgments

We are grateful to Prof. J.R. Schrock (Emporia State University, USA) for revising the manuscript.

Appendix A. Supporting information

Supplementary data associated with this article can be found in the online version at doi:10.1016/j.jhazmat.2020.124612.

References

Abbott, W.S., 1987. A method of computing the effectiveness of an insecticide. 1925. J. Am. Mosq. Control Assoc. 3, 302–303.

Alon, M., Alon, F., Nauen, R., Morin, S., 2008. Organophosphates' resistance in the B-biotype of *Bemisia tabaci* (Hemiptera: Aleyrodidae) is associated with a point mutation in an ace1-type acetylcholinesterase and overexpression of carboxylesterase. Insect Biochem. Mol. Biol. 38, 940–949.

Arthropod Pesticide Resistance Database, APRD 2019. ⟨https://www.pesticidere-sistance.org/⟩. (Accessed on 7 December 2019).

Bai, L.S., Zhao, C.X., Xu, J.J., Feng, C., Li, Y.Q., Dong, Y.L., Ma, Z.Q., 2019. Identification and biochemical characterization of carboxylesterase 001G associated with insecticide detoxification in *Helicoverpa armigera*. Pestic. Biochem Physiol. 157, 69–79.

Bauer, M.R., Mackey, M.D., 2019. Electrostatic complementarity as a fast and effective tool to optimize binding and selectivity of protein-ligand complexes. J. Med. Chem. 62, 3036–3050.

Baxter, C.A., Murray, C.W., Clark, D.E., Westhead, D.R., Eldridge, M.D., 1998. Flexible docking using Tabu search and an empirical estimate of binding affinity. Proteins 33, 367–382.

Bizzaro, D., Mazzoni, E., Barbolini, E., Giannini, S., Cassanelli, S., Pavesi, F., Cravedi, P., Manicardi, G.C., 2005. Relationship among expression, amplification, and methylation of FE4 esterase genes in Italian populations of *Myzus persicae* (Sulzer) (Homoptera: Aphididae). Pestic. Biochem. Physiol. 81, 51–58.

Campbell, P.M., Newcomb, R.D., Russell, R.J., Oakeshott, J.G., 1998. Two different amino acid substitutions in the ali-esterase, E3, confer alternative types of organophosphorus insecticide resistance in the sheep blowfly, *Lucilia cuprina*. Insect Biochem. Mol. Biol. 28, 139–150.

Cao, C.W., Zhang, J., Gao, X.W., Liang, P., Guo, H.L., 2008. Differential mRNA expression levels and gene sequences of carboxylesterase in both deltamethrin resistant and susceptible strains of the cotton aphid, *Aphis gossypii*. Insect Sci. 15, 209–216.

de Carvalho, R.A., Torres, T.T., de Azeredo-Espin, A.M.L., 2006. A survey of mutations in the *Cochliomyia hominivorax* (Diptera: Calliphoridae) esterase E3 gene associated with organophosphate resistance and the molecular identification of mutant alleles. Vet. Parasitol. 140, 344–351.

Case, D., Darden, T., Cheatham III, T., Simmerling, C., Wang, J., Duke, R., Luo, R., Walker, R., Zhang, W., Merz, K., 2010. AMBER 12, 2012. University of California,, San Francisco, pp. 1–826, 2012.

Cheeseright, T., Mackey, M., Rose, S., Vinter, A., 2006. Molecular field extrema as descriptors of biological activity: definition and validation. J. Chem. Inf. Model. 46, 665–676.

Chen, V.B., Arendall, W.B., Headd, J.J., Keedy, D.A., Immormino, R.M., Kapral, G.J., Murray, L.W., Richardson, J.S., Richardson, D.C., 2010. MolProbity: all-atom structure validation for macromolecular crystallography. Acta Crystallogr. Sect. D -Struct. Biol. 66, 12–21.

Chen, X., Liu, J., Zhang, Y., 2014. Cantharidin impedes the activity of protein serine/threonine phosphatase in *Plutella xylostella*. Mol. Biosyst. 10, 240–250.

Claudianos, C., Russell, R.J., Oakeshott, J.G., 1999. The same amino acid substitution in orthologous esterases confers organophosphate resistance on the house fly and a blowfly. Insect Biochem. Mol. Biol. 29, 675–686.
Cui, F., Qu, H., Cong, J., Liu, X.L., Qiao, C.L., 2007. Do mosquitoes acquire organophosphate resistance by functional changes in carboxylesterases? FASEB J. 21, 3584–3591.
W.L. DeLano, The PyMOL molecular graphics system, ⟨http://www.pymol.org⟩, (2002).
Eldridge, M.D., Murray, C.W., Auton, T.R., Paolini, G.V., Mee, R.P., 1997. Empirical scoring functions: I. The development of a fast empirical scoring function to estimate the binding affinity of ligands in receptor complexes. J. Comput. Aided Mol. Design 11, 425–445.
Feng, X.C., Li, M., Liu, N.N., 2018. Carboxylesterase genes in pyrethroid resistant house flies, *Musca domestica*. Insect Biochem. Mol. Biol. 92, 30–39.
Flare, 4.0.2, Cresset®, Litlington, Cambridgeshire, UK, ⟨http://www.cresset-group.com/flare/⟩.
Food and Agriculture Organization (FAO), ⟨http://faostat3.fao.org/search/pyrethroid/E⟩ (Accessed on 20th October, 2020).
Furlong, M.J., Wright, D.J., Dosdall, L.M., 2013. Diamondback moth ecology and management: problems, progress, and prospects. In: Berenbaum, M.R. (Ed.), Annual Review of Entomology, Vol 58. Annual Reviews, Palo Alto, p. 517 (+).
Gong, Y.H., Ai, G.M., Li, M., Shi, X.Y., Diao, Q.Y., Gao, X.W., 2017. Functional characterization of carboxylesterase gene mutations involved in *Aphis gossypii* resistance to organophosphate insecticides. Insect Mol. Biol. 26, 702–714.
Grant, D.F., Bender, D.M., Hammock, B.D.J., 1989. Quantitative kinetic assays for glutathione S-transferase and general esterase in individual mosquitoes using an EIA reader. Insect Biochem. 19, 741–751.
Gu, Z.Y., Sun, S.S., Wang, Y.H., Wang, B.B., Xie, Y., Ma, L., Wang, J.M., Shen, W.D., Li, B., 2013. Transcriptional characteristics of gene expression in the midgut of domestic silkworms (*Bombyx mori*) exposed to phoxim. Pestic. Biochem. Physiol. 105, 36–43.
Hanh Thi, D., Kadokami, K., Pan, S., Matsuura, N., Trung Quang, N., 2014. Screening and analysis of 940 organic micro-pollutants in river sediments in Vietnam using an automated identification and quantification database system for GC-MS. Chemosphere 107, 462–472.
Han, Y.C., Wu, S.W., Li, Y.P., Liu, J.W., Campbell, P.M., Farnsworth, C., Scott, C., Russell, R.J., Oakeshott, J.G., Wu, Y.D., 2012. Proteomic and molecular analyses of esterases associated with monocrotophos resistance in *Helicoverpa armigera*. Pestic. Biochem. Physiol. 104, 243–251.
Hartley, C.J., Newcomb, R.D., Russell, R.J., Yong, C.G., Stevens, J.R., Yeates, D.K., La Salle, J., Oakeshott, J.G., 2006. Amplification of DNA from preserved specimens shows blowflies were preadapted for the rapid evolution of insecticide resistance. Proc. Natl. Acad. Sci. 103, 8757–8762.
Hummer, G., Rasaiah, J.C., Noworyta, J.P., 2001. Water conduction through the hydrophobic channel of a carbon nanotube. Nature 414, 188–190.
Jakalian, A., Jack, D.B., Bayly, C.I., 2002. Fast, efficient generation of high-quality atomic charges. AM1-BCC model: II. Parameterization and validation. J. Comput. Chem. 23, 1623–1641.
Jones, G., Willett, P., Glen, R.C., 1995. Molecular recognition of receptor sites using a genetic algorithm with a description of desolvation. J. Mol. Biol. 245, 43–53.
Jones, G., Willett, P., Glen, R.C., Leach, A.R., Taylor, R., 1997. Development and validation of a genetic algorithm for flexible docking. J. Mol. Biol. 267, 727–748.
Kuhn, M., Firth-Clark, S., Tosco, P., Mey, A.S.J.S., Mackey, M., Michel, J., 2020. Assessment of binding affinity via alchemical free-energy calculations. J. Chem. Inf. Model. 60, 3120–3130.
Lan, W.S., Cong, J., Jiang, H., Jiang, S.R., Qiao, C.L., 2005. Expression and characterization of carboxylesterase E4 gene from peach-potato aphid (*Myzus persicae*) for degradation of carbaryl and malathion. Biotechnol. Lett. 27, 1141–1146.
Liu, T.X., Hutchinson, W.D., Chen, W., Burkness, E.C., 2003. Comparative susceptibilities of diamondback moth (Lepidoptera: Plutellidae) and cabbage looper (Lepidoptera: Noctuidae) from Minnesota and South Texas to lambda-cyhalothrin and indoxacarb. J. Econ. Entomol. 96, 1230–1236.
Liu, J., Li, Y., Tian, Z., Sun, H., Chen, Xe, Zheng, S., Zhang, Y., 2018. Identification of Key Residues associated with the interaction between *Plutella xylostella* sigma-class glutathione s-transferase and the inhibitor s-hexyl glutathione. J. Agric. Food Chem. 66, 10169–10178.
Liu, M.Y., Tzeng, Y.J., Sun, C.N., 1981. Diamondback moth resistance to several synthetic pyrethroids. J. Econ. Entomol. 74, 393–396.
Liu, J., Yang, X., Zhang, Y., 2014. Characterization of a lambda-cyhalothrin metabolizing glutathione S-transferase CpGSTd1 from *Cydia pomonella* (L.). Appl. Microbiol. Biotechnol. 98, 8947–8962.
Livak, K.J., 2001. Analysis of relative gene expression data using real-time quantitative PCR and the $2^{-\Delta\Delta CT}$ method. Methods 25, 402–408.
Li, Y., Bai, L., Zhao, C., Xu, J., Sun, Z., Dong, Y., Li, D., Liu, X.L., Ma, Z.Q., 2020. Functional characterization of two carboxylesterase genes involved in pyrethroid detoxification in *Helicoverpa armigera*. J. Agric. Food Chem. 68, 3390–3402.
Li, H., Cheng, F., Wei, Y., Lydy, M.J., You, J., 2017. Global occurrence of pyrethroid insecticides in sediment and the associated toxicological effects on benthic invertebrates: an overview. J. Hazard. Mater. 324, 258–271.
Li, X.C., Schuler, M.A., Berenbaum, M.R., 2007. Molecular mechanisms of metabolic resistance to synthetic and natural xenobiotics. Annu. Rev. Entomol. 52, 231–253.
Long, J.L.A., House, W.A., Parker, A., Rae, J.E., 1998. Micro-organic compounds associated with sediments in the Humber rivers. Sci. Total Environ. 210, 229–253.
Lu, F.G., Fu, K.Y., Li, Q., Guo, W.C., Ahmat, T., Li, G.Q., 2015. Identification of carboxylesterase genes and their expression profiles in the Colorado potato beetle *Leptinotarsa decemlineata* treated with fipronil and cyhalothrin. Pestic. Biochem. Physiol. 122, 86–95.
Lyubimov, A.V., Encyclopedia of Drug Metabolism and Interactions || Carboxylesterases, (2011).
C.J.W. Maa, H.J. Wang, C.F. Liu, Variation in carboxylesterase frequency and insecticide resistance of *Plutella xylostella* (L.) as a response to environmental gradients, (2001). In N.M. Endcrsby & P.M. Ridland (cds.), Proceedings of the 4th International Workshop on the Management of Diamondback Moth and other Crucifer Pests. Melbourne, Australia, November 26–29, 2001.
Mouches, C., Pasteur, N., Berge, J.B., Hyrien, O., Raymond, M., de Saint Vincent, B.R., de Silvestri, M., Georghiou, G.P., 1986. Amplification of an esterase gene is responsible for insecticide resistance in a California *Culex* mosquito. Science 233, 778–780.
Newcomb, R.D., Campbell, P.M., Ollis, D.L., Cheah, E., Russell, R.J., Oakeshott, J.G., 1997. A single amino acid substitution converts a carboxylesterase to an organophosphorus hydrolase and confers insecticide resistance on a blowfly. Proc. Natl. Acad. Sci. 94, 7464–7468.
Oakeshott, J.G., Farnsworth, C.A., East, P.D., Scott, C., Han, Y.C., Wu, Y.D., Russell, R.J., 2013. How many genetic options for evolving insecticide resistance in heliothine and spodopteran pests? Pest Manag. Sci. 69, 889–896.
Oakeshott, J.G., Johnson, R.M., Berenbaum, M.R., Ranson, H., Cristino, A.S., Claudianos, C., 2010. Metabolic enzymes associated with xenobiotic and chemosensory responses in *Nasonia vitripennis*. Insect. Mol. Biol. 19, 147–163.
Ray, D.E., Fry, J.R., 2006. A reassessment of the neurotoxicity of pyrethroid insecticides. Pharmacol. Ther. 111, 174–193.
Sayyed, A.H., Saeed, S., Noor-Ul-Ane, M., Crickmore, N., 2008. Genetic, biochemical, and physiological characterization of spinosad resistance in *Plutella xylostella* (Lepidoptera: Plutellidae). J. Econ. Entomol. 101, 1658–1666.
Schrag, J.D., Cygler, M., 2004. Defining substrate characteristics from 3D structure: perspective on EstA structure. Structure 12, 521–522.
Shelton, A.M., Wyman, J.A., Cushing, N.L., Apfelbeck, K., Dennehy, T.J., Mahr, S.E.R., Eigenbrode, S.D., 1993. Insecticide resistance of diamondback moth (Lepidoptera, Plutellidae) In North-America. J. Econ. Entomol. 86, 11–19.
Soderlund, D.M., 2008. Pyrethroids, knockdown resistance and sodium channels. Pest Manag. Sci. 64, 610–616.
Sun, J.Y., Liang, P., Gao, X.W., 2012. Cross-resistance patterns and fitness in fufenozide-resistant diamondback moth, *Plutella xylostella* (Lepidoptera: Plutellidae). Pest Manag. Sci. 68, 285–289.
Šali, A., Blundell, T.L., 1993. Comparative protein modelling by satisfaction of spatial restraints. J. Mol. Biol. 234, 779–815.
Teese, M.G., Farnsworth, C.A., Li, Y.Q., Coppin, C.W., Devonshire, A.L., Scott, C., East, P., Russell, R.J., Oakeshott, J.G., 2013. Heterologous expression and biochemical characterisation of fourteen esterases from *Helicoverpa armigera*. PLoS One 8, e65951.
Tian, Z., Liu, J., Zhang, Y., 2016a. Key residues involved in the interaction between *Cydia pomonella* pheromone binding protein 1 (CpomPBP1) and Codlemone. J. Agric. Food Chem. 64, 7994–8001.
Tian, Z., Liu, J., Zhang, Y., 2016b. Structural insights into *Cydia pomonella* pheromone binding protein 2 mediated prediction of potentially active semiochemicals. Sci. Rep. 6, 22336.
Tian, Z., Li, Y., Xing, Y., Li, R., Liu, J., 2019. Structural Insights into two representative conformations of the complex formed by *Grapholita molesta* (Busck) pheromone binding protein 2 and Z-8-dodecenyl acetate. J. Agric. Food Chem. 67, 4425–4434.
Tian, Z., Li, Y., Zhou, T., Ye, X., Li, R.C., Liu, J.Y., 2020. Structure dynamics reveal key residues essential for the sense of 1-dodecanol by Cydia pomonellapheromone binding protein 2 (CpomPBP2). Pest Manag. Sci. 76, 3667–3675.
Tsubota, T., Shiotsuki, T., 2010. Genomic analysis of carboxyl/cholinesterase genes in the silkworm *Bombyx mori*. BMC Genom. 11, 377.
Vontas, J., Blass, C., Koutsos, A., David, J.P., Kafatos, F., Louis, C., Hemingway, J., Christophides, G., Ranson, H., 2005. Gene expression in insecticide resistant and susceptible *Anopheles gambiae* strains constitutively or after insecticide exposure. Insect. Mol. Biol. 14, 509–521.
Wang, K., Huang, Y.N., Li, X.Y., Chen, M.H., 2018. Functional analysis of a carboxylesterase gene associated with isoprocarb and cyhalothrin resistance in *Rhopalosiphum padi* (L.). Front. Physiol. 9, 11.
Wang, J., Wolf, R.M., Caldwell, J.W., Kollman, P.A., Case, D.A., 2004. Development and testing of a general amber force field. J. Comput. Chem. 25, 1157–1174.
Wan, C., Hao, Z.X., Feng, X.Q., 2016. Structures, properties, and energy-storage mechanisms of the semi-lunar process cuticles in locusts. Sci. Rep. 6, 35219.
Wheelock, C.E., Shan, G., Ottea, J., 2005. Overview of carboxylesterases and their role in the metabolism of insecticides. J. Pestic. Sci. 30, 75–83.
Yi, C.G., Hieu, T.T., Lee, S.H., Choi, B.R., Kwon, M., Ahn, Y.J., 2016. Toxicity of Lavandula angustifolia oil constituents and spray formulations to insecticide-susceptible and pyrethroid-resistant *Plutella xylostella* and its endoparasitoid *Cotesia glomerata*. Pest Manag. Sci. 72, 1202–1210.
Yu, Q.Y., Lu, C., Li, W.L., Xiang, Z.H., Zhang, Z., 2009. Annotation and expression of carboxylesterases in the silkworm, Bombyx mori. BMC Genom. 10, 553.
Yu, S.J., Nguyen, S.N., 1992. Detection and biochemical-characterization of insecticide resistance in the diamondback moth. Pestic. Biochem. Physiol. 44, 74–81.
Zhang, J.Q., Li, D.Q., Ge, P.T., Yang, M.L., Guo, Y.P., Zhu, K.Y., Ma, E.B., Zhang, J.Z., 2013. RNA interference revealed the roles of two carboxylesterase genes in insecticide detoxification in *Locusta migratoria*. Chemosphere 93, 1207–1215.
Zhang, L., Shi, J., Shi, X.Y., Liang, P., Gao, J.P., Gao, X.W., 2010. Quantitative and qualitative changes of the carboxylesterase associated with beta-cypermethrin

resistance in the housefly, *Musca domestica* (Diptera: Muscidae). Comp. Biochem. Physiol. B-Biochem. Mol. Biol. 156, 6–11.
Zhou, L.J., Huang, J.G., Xu, H.H., 2011. Monitoring resistance of field populations of diamondback moth *Plutella xylostella* L. (Lepidoptera: Yponomeutidae) to five insecticides in South China: A ten-year case study. Crop Prot. 30, 272–278.
Zhu, B., Shan, J.Q., Li, R., Liang, P., Gao, X.W., 2019. Identification and RNAi-based function analysis of chitinase family genes in diamondback moth, *Plutella xylostella*. Pest Manag. Sci. 75, 1951–1961.